Vol 18 No 11, November 2009
1674-1056/2009/18(11)/4846-06

Chinese Physics B

© 2009 Chin. Phys. Soc.
and IOP Publishing Ltd

High order correlation–polarization potential for vibrational excitation scattering of diatomic molecules by low-energy electrons*

Feng Hao(冯 灏)[a)†], Sun Wei-Guo(孙卫国)[a)b)], and Zeng Yang-Yang(曾阳阳)[b)]

[a)] *School of Physics and Chemistry, Xihua University, Chengdu* 610039, *China*

[b)] *Institute of Atomic and Molecular Physics, Sichuan University, Chengdu* 610065, *China*

(Received 24 September 2008; revised manuscript received 24 February 2009)

This paper introduces a correlation–polarization potential with high order terms for vibrational excitation in electron–molecule scattering. The new polarization potential generalizes the two-term approximation so that it can better reflect the dependence of correlation and polarization effects on the position coordinate of the scattering electron. It applies the new potential on the vibrational excitation scattering from N_2 in an energy range which includes the $^2\Pi_g$ shape resonance. The good agreement of theoretical resonant peaks with experiments shows that polarization potentials with high order terms are important and should be included in vibrational excitation scattering.

Keywords: vibrational excitation scattering, correlation–polarization, high order, resonant
PACC: 3480G

1. Introduction

Interaction between an incident electron and a target has been a challenge to the theoretical study of low-energy electron scattering from atoms and molecules. As the electron is detected beyond the asymptotic region, it is influenced by the non-spherical potential field produced by a multi-centred target having internal degrees of freedom of rotational and vibrational motions. While the electron approaches the target, it is indistinguishable from the target electrons. In particular, inside the core region, the bound–free correlation effects plus the exchange effects imposed by the quantum mechanical feature dominate the cross sections.

Full quantum-mechanical treatment of the interaction between the low-energy electron and the target is very hard and often impractical. Nevertheless, a partitioning of static, exchange and correlation–polarization is useful in theoretical study.[1,2] Of the three interaction contributions, inclusion of electrostatic effects by averaging the Coulomb potential energy over a Hartree–Fock probability density for the target is routine.[3,4] Meanwhile, the exchange effects can be included either rigorously[5−8] or via a variety of well-established local model potentials.[9−11]

Rigorous quantum mechanical treatment of correlation and polarization effects is formally straightforward but impossible to implement without approximation. In the vibrational excitation scattering of diatomic molecules by low-energy electrons, 'better-than-adiabatic dipole (BTAD) potential'[12−14] and 'distributed spherical Gaussian (DSG) potential'[15−17] have been applied to e–H_2 and e–N_2. Both of them mimic the many-body correlation effects via a local model only dependent on the distance between the incident electron and the target. BTAD entails variational calculations on the electron–molecule system in the field of a fixed projectile.[18,19] The DSG potential models the scattering electron by a spherical charge density which decays with radial distance from its origin at the (fixed) electron position r_e.[15,20]

Both BTAD and DSG potentials can be applied to describe the $^2\Pi_g$ shape resonance in e–N_2, in which the resonance energy and width are critically dependent on the short-range electron–molecule interaction.[13,21−26] However, BTAD and DSG potentials are based on the two-term approximation and are calculated only in parallel and perpendicular directions of the incident electron. Since N_2 has a strong non-spherical feature, the high order terms of the polarization potential play an important role. Moreover, v_0 and v_2 are weakened by the two-term approxima-

*Project supported by National Natural Science Foundation of China (Grant Nos 10504022 and 10774105).
†Corresponding author. E-mail: fenghao@mail.xhu.edu.cn

tion and the exchange potential has to be tuned to ensure the proper resonant peak. If the converged 'exact' exchange potential is used, the two-term polarization potentials 'shift' the resonant energy higher.

We report here a generalization of the two-term polarization potential to include high order terms. In Section 2 we give the equations of high order polarization potentials and summarize the scattering theory which we used to calculate vibrational excitation cross sections. Then we apply the new polarization potentials for the resonant e–N_2 scattering and compare the cross sections with those of the two-term approximation in Section 3. A brief discussion of the present work is summarized in Section 4.

2. Theory

2.1. High order polarization

In a theoretical study of low-energy scattering, the local terms in $V^{\rm int}$, the sum of the static and (model) correlation/polarization potentials, are usually expanded in Legendre polynomials,[27,28]

$$V^{\rm scp}(\boldsymbol{r}) \equiv V^{\rm st}(\boldsymbol{r}) + V^{\rm cp}(\boldsymbol{r}) = \sum_{\lambda=0}^{\infty} v_\lambda^{\rm scp}(r) P_\lambda(\cos\theta), \tag{1}$$

where $\boldsymbol{r}$ is the radial coordinate of the scattering electron, and θ the angle between $\boldsymbol{r}$ and the internuclear axis $\boldsymbol{R}$. The static potential $V^{\rm st}$, is usually expanded as high order Legendre polynomials. For example, λ is from 0 up to 6 for e–H_2 and up to 14 for e–N_2 respectively. Meanwhile, only two terms $v_0^{\rm cp}(r)$ and $v_2^{\rm cp}(r)$ are retained in the $V^{\rm cp}$ approximately.

For a diatomic molecule, to determine $v_0^{\rm cp}(r)$ and $v_2^{\rm cp}(r)$, $V^{\rm cp}$ is calculated at only two angles, $\theta_e = 0$ and $\pi/2$. Then,

$$v_0^{\rm cp}(r) = \frac{1}{3}\left[2v_{x_{\rm e}}^{\rm cp} + v_{z_{\rm e}}^{\rm cp}\right], \tag{2a}$$

$$v_2^{\rm cp}(r) = \frac{2}{3}\left[v_{x_{\rm e}}^{\rm cp} - v_{z_{\rm e}}^{\rm cp}\right]. \tag{2b}$$

In previous research, BTAD and DSG polarization potentials are calculated through Eq.(2).[12,13,15,28]

The two-term approximation is valid for weakly non-spherical targets. However, N_2 has a strong non-spherical feature. Moreover, the DSG potential is more dependent on the incident angles than BTAD since the exponential factor of DSG is a function of the incident angle.[15] Inclusion of $\theta_{\rm e} = 0$ and $\pi/2$ only is not enough. So the high order of $v_\lambda^{\rm cp}(r)$ should be included.

$$V^{\rm cp}(\boldsymbol{r}) = \sum_{\lambda=0}^{\lambda_{\max}} v_\lambda^{\rm cp}(r) P_\lambda(\cos\theta). \tag{3}$$

Using the orthogonality of the Legendre polynomials, we can obtain

$$v_\lambda^{\rm cp}(r) = \frac{2\lambda+1}{2}\int_0^{\pi} V^{\rm cp}(\boldsymbol{r}) P_\lambda(\cos\theta)\sin\theta\,{\rm d}\theta, \tag{4}$$

where $\boldsymbol{r} = (r\sin\theta, 0, r\cos\theta)$. To simplify the calculation for a homo-nuclear molecule, we substitute θ by $\alpha = \theta - \pi/2$, then

$$v_\lambda^{\rm cp}(r) = \frac{2\lambda+1}{2}\int_{-\pi/2}^{\pi/2} V^{\rm cp}(r\cos\alpha, 0, -r\sin\alpha) P_\lambda[\cos(\alpha+\pi/2)]\cos\alpha\,{\rm d}\alpha, \tag{5}$$

and further

$$\begin{aligned} v_\lambda^{\rm cp}(r) = \frac{2\lambda+1}{2}\int_0^{\pi/2} {\rm d}\alpha \{ & V^{\rm cp}(r\cos\alpha, 0, -r\sin\alpha) P_\lambda[\cos(\alpha+\pi/2)] \\ & + V^{\rm cp}(r\cos\alpha, 0, r\sin\alpha) P_\lambda[\cos(-\alpha+\pi/2)]\}. \end{aligned} \tag{6}$$

This integral could be easily evaluated by Gauss–Legendre (GL) quadratures.[29,30] Since for a homo-nuclear molecule, $V^{\rm cp}(r\cos\alpha, 0, -r\sin\alpha)$ is equal to $V^{\rm cp}(r\cos\alpha, 0, r\sin\alpha)$, a smaller number of quadratures can converge.

An additional advantage of GL quadratures is that we can avoid the singularity when the incident electron approaches the nucleus. Under the two-term approximation, we have to jump over r close to the nucleus at which the interaction is infinity. By using GL quadratures, θ can be chosen not equal to 0 so the incident electron will not approach exactly the position of the nucleus.

2.2. Scattering theory

For vibrational excitation scattering, the collision processes are treated on the fixed nuclear orientation approximation,[31,32] in which one can ignore the rotational kinetic-energy operator in the target molecule Hamiltonian and average over molecule orientations in the calculation while vibrational effects are fully considered by using a vibrational state expansion procedure on the wavefunction of the system. Thus, the collision dynamics are based on the body-frame-vibrational close-coupling (BFVCC) method[27] which is the strategy used in this study.

This method proceeds in two steps. First, the wavefunction of the system is projected onto the ground Born–Oppenheimer electronic state of the target. Then, the resulting scattering function can be expanded into the complete set $\{\phi_v(R)Y_\ell^\Lambda(\hat{r})\}$, where $\phi_v(R)$ are the vibrational wavefunctions of the target, and the spherical harmonics $Y_\ell^\Lambda(\hat{r})$ are the angular functions. The latter are labelled by quantum numbers ℓ for the orbital angular momentum of the electron and Λ for the projection of this angular momentum on the internuclear axis. The entrance-channel is denoted by subscript 0 and exit-channel by the subscript v. Accordingly, the integral–differential equation of BFVCC can be expressed as follows:

$$\left[-\frac{1}{2}\frac{\mathrm{d}^2}{\mathrm{d}r_\mathrm{e}^2}+\frac{\ell(\ell+1)}{2r_\mathrm{e}^2}+V^\Lambda_{v\ell,v\ell(r)}-\frac{1}{2}k_v^2\right]u^\Lambda_{v\ell,v_0\ell_0}(r_\mathrm{e}) = \sum_{v',\ell'\neq v,\ell} V^\Lambda_{v\ell,v'\ell'}(r)u^\Lambda_{v'\ell',v_0\ell_0}(r_\mathrm{e}). \quad (7)$$

Here $k_v^2/2$ is the exit-channel energy, determined by energy conservation as

$$\frac{1}{2}k_v^2=\frac{1}{2}k_0^2-(\epsilon_v-\epsilon_0), \quad (8)$$

where ϵ_v is the energy of the v^{th} vibrational state. The matrix elements of the interaction potential energy can be expressed as

$$V^\Lambda_{v\ell,v'\ell'}(r)=\langle v,\ell;\Lambda|V^{\mathrm{scp}}(r)|v',\ell';\Lambda\rangle_{R,\hat{r}_\mathrm{e}}. \quad (9)$$

The coupling element is expressed as in Eq.(1) where the Legendre projections include static, exchange, and correlation–polarization contributions to sufficient maximum order $\lambda_{\max}$ to converge the desired scattering quantities.

The structure of the coupling total interaction potential is now performed as

$$V^\Lambda_{v\ell,v'\ell'}(r)=\sum_{\lambda=0}^{\lambda_{\max}} g_\lambda(ll';\Lambda)\omega^\lambda_{v,v'}(r), \quad (10a)$$

where the angular coupling coefficients, written in terms of Clebsch–Gordan coefficients by using the conventions of Rose,[33] are simply

$$g_\lambda(\ell,\ell';\Lambda)=\left(\frac{2\ell'+1}{2\ell+1}\right)^{1/2}C(\ell'\lambda\ell;\Lambda 0)C(\ell'\lambda\ell;00). \quad (10b)$$

and the radial vibrational coupling potential, expressed in terms of Legendre projections $v_\lambda(r,R)$ of the interaction potential, is

$$\omega^\lambda_{v,v'}(r)=\langle\phi_v(R)|v_\lambda(r_\mathrm{e},R)|\phi_{v'}(R)\rangle. \quad (10c)$$

2.3. Implementation

We implemented a subroutine to calculate DSG potentials by using the GAMESS package.[15,34] To calculate a DSG potential with high order terms (DSGH), GL quadratures are used firstly to partition the incident electron to different incident directions at a fixed scattering distance. Then for every incident direction, the DSG potential is calculated. Finally, GL quadratures are used again to calculate the integral as Eq.(6). In this study, 20 GL quadratures are used to get the converged integrals.

We evaluated the interaction potential at the following values of R: 1.60, 1.70, 1.80, 1.85, 1.90, 1.95, 2.00, 2.02 (the equilibrium internuclear separation for our Hartree–Fock electronic wavefunction), 2.068, 2.10, 2.20, 2.30, 2.40 and $2.50a_0$.

The solution of the BFVCC equation as Eq.(7) is evaluated to calculate the vibrational excitation scattering. Apart from the static and DSG/DSGH polarization potentials, 'tuned-free-electron-gas-exchange (TFEGE)' is used as the local exchange term. Firstly, a rigid rotor calculation is performed by including the rigorous exchange operator. Then TFEGE is tuned to reproduce the resonant energy as that with 'exact' exchange at the same nuclear distance. In the previous research, the rigorous exchange potential is calculated only through 51 GL quadratures. If more GL quadratures are used, DSG (and BTAD) will shift the resonant energy higher. However, to get the converged cross sections, 200 or more GL quadratures should be used. In this study, we use 212 GL quadratures to calculate the rigid rotor cross sections with static, DSG/DSGH and 'exact' exchange potentials. Then TFEGE is tuned to reproduce the resonant energy for every nuclear distance.

To get a converged K matrix, 15 vibrational functions and 11 partial waves are used in our study.

3. Results

We calculate DSGH polarization potentials of e–H_2 and e–N_2 and compare them with DSG potentials (only two terms included) in Fig.1 and Fig.2.

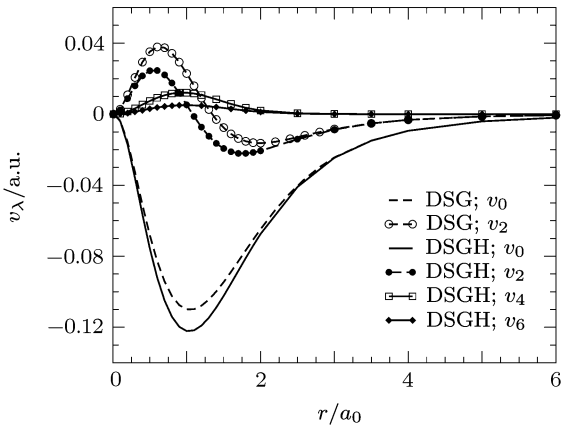


Fig.1. Comparison between DSGH and DSG potentials of e–H_2 at $R = 1.40\,a_0$.

From Figs.1 and 2, we see that DSG potentials weaken v_0 and v_2 for both e–H_2 and e–N_2. More importantly, v_λ are not converged until $\lambda > 6$. So in our research, 6 and 14 terms are retained in polarization potentials for e–H_2 and e–N_2 respectively as in static potentials.

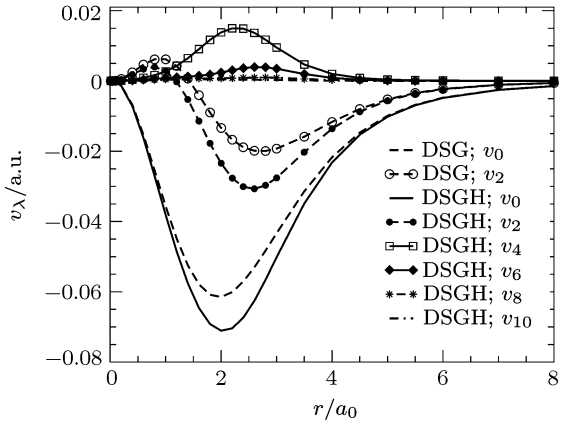


Fig.2. Comparison between DSGH and DSG potentials of e–N_2 at $R = 2.02\,a_0$

Using the new DSGH potentials, we calculate the cross sections of e–H_2 and e–N_2 based on the rigid rotor model with inclusion of the 'exact' exchange potential at equilibrium distances. The results are plotted in Figs.3 and 4.

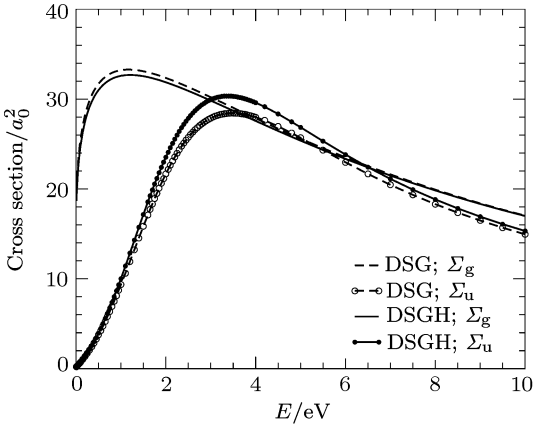


Fig.3. Comparison between cross sections based on DSGH and DSG potentials of e–H_2 at $R = 1.40\,a_0$ (rigid rotor).

For e–H_2 scattering, Σ_g and Σ_u are dominant in the total cross sections. The magnitudes of Σ_u cross sections with DSGH are larger than those with DSG, while the Σ_g cross sections are slightly different.

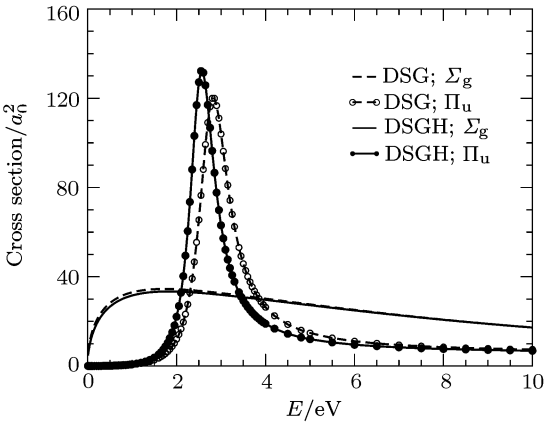


Fig.4. Comparison between cross sections based on DSGH and DSG potentials of e–N_2 at $R = 2.02\,a_0$ (rigid rotor).

For e–N_2 scattering, although the cross sections of Σ_g differ little for the DSG and DSGH potentials, the resonant energy of Π_g with the DSG potential shifts higher than that with DSGH. Since Π_g has the most important contribution to the total cross sections in the resonant region, DSGH and DSG will generate different positions and magnitudes of the resonant peaks.

Based on the BFVCC equation as Eq.(7), the total vibrational excitation cross sections of e–N_2 are calculated. The results are compared in Fig.5. We see that by using both DSG and BTAD polarization potentials the resonant peaks are shifted higher, while DSGH can offset this discrepancy. The integral cross

section (ICS) based on the DSGH polarization potential agrees well with the experimental data in the resonant region, especially for the first four resonant peaks. Although the theoretical magnitudes are a little higher than the experimental data, the positions of the peaks are in good agreement.

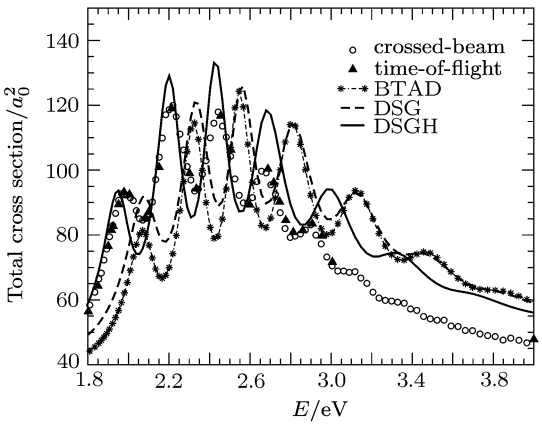


Fig.5. Total vibrational excitation cross sections of e–N_2. Crossed-beam is from Ref.[35] and time-of-flight is from Ref.[28].

Moreover, we compute the elastic ($0 \to 0$) and inelastic ($0 \to 1$) vibrational differential cross sections of different polarization potentials at energies below the resonant region (0.80 and 1.50 eV) and compare them with the latest experiments from Fig.6 to Fig.9.

From Figs.6 and 7, we see both DSG and DSGH polarization potentials greatly improve the BTAD potential for elastic scattering at angles less than 100 degrees. The DSG and DSGH potentials, however, give nearly same differential cross sections (DCSs).

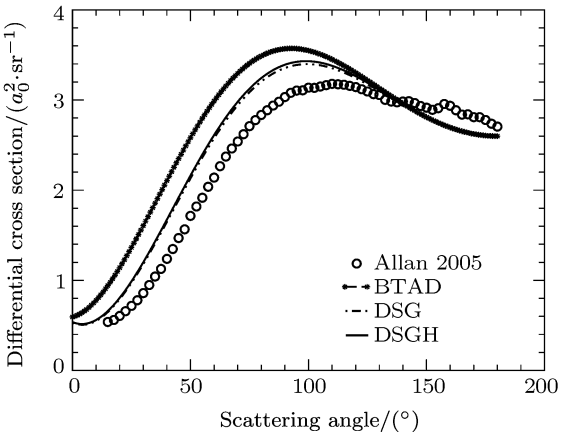


Fig.6. Elastic ($0 \to 0$) differential cross sections of e–N_2 at 0.80 eV. Experimental DCS (○) is from Ref.[36].

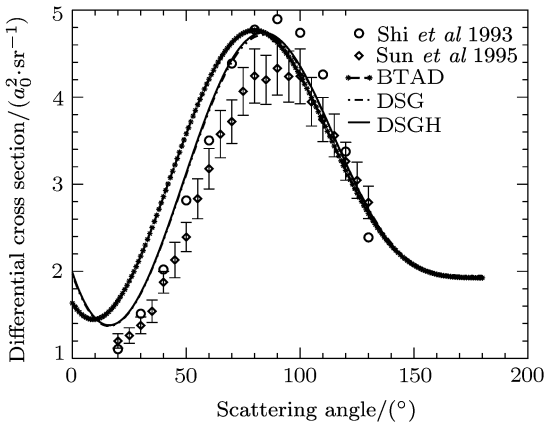


Fig.7. Elastic ($0 \to 0$) differential cross sections of e–N_2 at 1.50 eV. Experimental DCS (○) is from Ref.[37] and (◇) is from Ref.[28].

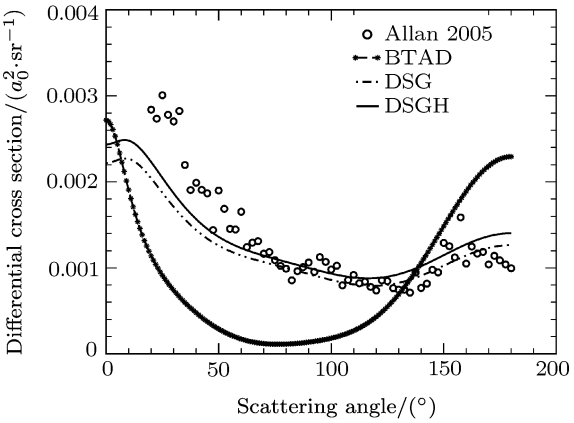


Fig.8. Inelastic ($0 \to 1$) differential cross sections of e–N_2 at 0.80 eV. Experimental DCS (○) is from Ref.[36].

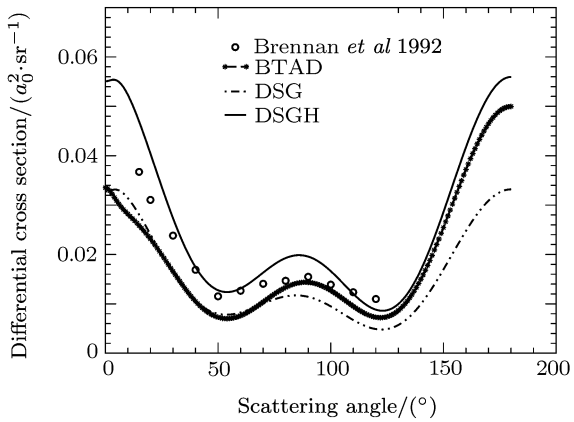


Fig.9. Inelastic ($0 \to 1$) differential cross sections of e–N_2 at 1.50 eV. Experimental DCS (○) is from Ref.[38].

For inelastic vibrational scattering, on the other hand, DCSs of the DSGH polarization potential are different from those of the BTAD and DSG potentials. In Fig.6, DSG and DSGH improve DCSs in the whole

incident angles. Although DSG corrects the DCSs of BTAD at incident angles less than 120 degrees, the DCSs of DSGH are a little closer to Allan's experimental data[36] than those of DSG at angles less than 60 degrees. At 1.5 eV, the inelastic DCSs of DSGH agree well with experimental data while the DCSs of both BTAD and DSG are lower from 0 to 180 degrees.

4. Conclusions

The comparisons between ICSs and DCSs of theoretical and experimental data reported here show that high order terms of polarization potentials are of importance in both resonant and non-resonant scattering. Since the DSG potential is dependent on the incident direction, the two-term approximation is not sufficient to describe its property in the whole space. DSGH, with higher order terms than DSG, however, shows that v_0 and v_2 are underestimated while higher order terms should be considered. By using DSGH and the converged exchange potential, the theoretical total vibrational cross sections agree well with the experimental data. The positions of the first four resonant peaks are reproduced.

Above 3.0 eV, although the DSGH ICS is closer to the experimental data, the theoretical calculations of BTAD, DSG and DSGH are all higher than both crossed-beam and time-of-flight data. Future research should be considered by improving the target charge density to get a more accurate interaction.

The comparisons beween elastic and inelastic differential cross sections of polarization potentials with experimental data argue that high order terms are important for inelastic vibrational scattering at low incident energies. Subsequent research will consider resonant excitations with high order polarization potentials.

Acknowledgment

The authors are grateful to Professor Michael A. Morrison (University of Oklahoma, USA) for his valuable suggestions and discussions.

References

[1] Lane N F 1980 *Rev. Mod. Phys.* **52** 29
[2] Morrison M A 1983 *Aust. J. Phys.* **36** 239
[3] Morrison M A 1980 *Comput. Phys. Commun.* **21** 63
[4] Schmid G B, Norcross D W and Collins L A 1980 *Comput. Phys. Commun.* **21** 79
[5] Trail W K 1991 *Exchange in Vibrational Excitation of Small Molecules by Electron Impact* Ph. D. Thesis (The University of Oklahoma, USA)
[6] Schneider B I and Collins L A 1981 *Phys. Rev.* A **24** 1264
[7] Collins L A and Schneider B I 1986 *Phys. Rev.* A **34** 1564
[8] Danby G, Elza B K and Morrison M A 1996 *J. Phys.* B **29** 2265
[9] Morrison M A and Collins L A 1978 *Phys. Rev.* A **17** 918
[10] Morrison M A and Collins L A 1981 *Phys. Rev.* A **23** 127
[11] Collins L A and Morrison M A 1982 *Phys. Rev.* A **25** 1764
[12] Gibson T L and Morrison M A 1984 *Phys. Rev.* A **29** 2497
[13] Morrison M A and Saha B C 1986 *Phys. Rev.* A **34** 2786
[14] Yu J Z, Feng H and Sun W G 2008 *Acta Phys. Sin.* **57** 4143 (in Chinese)
[15] Feng H, Sun W G and Morrison M A 2003 *Phys. Rev.* A **68** 062709
[16] Dai W, Sun W G, Feng H and Tang Y J 2007 *Mol. Phys.* **105** 2935
[17] Dai W, Sun W G, Feng H and Tang Y J, Shen L and Yu J Z 2008 *Acta Phys. Sin.* **57** 143 (in Chinese)
[18] Gibson T L 1982 *A Study of the Polarization Interaction with Application to Low-energy Electron-H_2 Callisions* Ph. D. Thesis (The University of Oklahoma, USA)
[19] Morrison M A, Saha B C and Gibson T L 1987 *Phys. Rev.* A **36** 3682
[20] Bouferguene A, Ema I and Weatherford C A 1999 *Phys. Rev.* A **59** 2712
[21] Bardsley J N and Mandl F 1962 *Rep. Prog. Phys.* **31** 471
[22] Krauss M and Mies F H 1970 *Phys. Rev.* A **1** 1592
[23] Schneider B I, Doumeuf M L and Lan V K 1979 *Phys. Rev. Lett.* **43** 1926
[24] Rescigno T N, Orel A E and McCurdy C W 1980 *J. Chem. Phys.* **73** 6347
[25] Hazi A U, Rescigno T N and Kurilla M 1981 *Phys. Rev.* A **23** 1089
[26] Gertitschke P L and Domcke W 1993 *J. Phys.* B **26** 2927
[27] Morrison M A and Sun W G 1995 *Computational Methods for Electron–Molecule Collisions* (New York: Plenum Publishing) p131
[28] Sun W G, Morrison M A, Isaacs W A, Trail W K, Alle D T, Gulley R J and Brennan M J 1995 *Phys. Rev.* A **52** 1229
[29] Stroud A H and Secrest D 1966 *Gaussian Quadrature Formulas* (Englewood Cliffs, N.J.: Prentice-Hall)
[30] Press W H, Teukolsky S A and Vetterling W T 1997 *Numerical Recipes in Fortran 77* Vol. **1** 2nd ed. (New York: Press Syndicate of the University of Cambridge)
[31] Feldt A N and Morrison M A 1984 *Phys. Rev.* A **29** 401
[32] Weatherford C A and Temkin A 1994 *Phys. Rev.* A **49** 2580
[33] Rose M E 1957 *Elementary Theory of Angular Momentum* (New York: John Wiley & Sons, Inc.)
[34] Schmidt M W, Baldridge K K, Boatz J A, Elbert S T, Gordon M S, Jensen J H, Koseki S, Matsunaga N, Nguyen K A, Su S J, *et al* 1993 *J. Comput. Chem.* **14** 1347
[35] Kennerly R E 1980 *Phys. Rev.* A **21** 1876
[36] Allan M 2005 *J. Phys.* B **38** 3655
[37] Shi X, Stephen T M and Burrow P D 1993 *J. Phys.* B **26** 121
[38] Brennan M J, Alle D T, Euripides P, Buckman S J and Brunger M J 1992 *J. Phys.* B **25** 2669